ACCOUNTS of chemical research

Article

Cite This: Acc. Chem. Res. 2018, 51, 960–969

pubs.acs.org/accounts

Orotidine 5′-Monophosphate Decarboxylase: Probing the Limits of the *Possible* for Enzyme Catalysis

John P. Richard,* Tina L. Amyes, and Archie C. Reyes

Department of Chemistry, University at Buffalo, SUNY, Buffalo, New York 14260-3000, United States

CONSPECTUS: The mystery associated with catalysis by what were once regarded as protein black boxes, diminished with the X-ray crystallographic determination of the three-dimensional structures of enzyme−substrate complexes. The report that several high-resolution X-ray crystal structures of orotidine 5′-monophosphate decarboxylase (OMPDC) failed to provide a consensus mechanism for enzyme-catalyzed decarboxylation of OMP to form uridine 5′-monophosphate, therefore, provoked a flurry of controversy. This controversy was fueled by the enormous 10^{23}-fold rate acceleration for this enzyme, which had "*jolted many biochemists' assumptions about the catalytic potential of enzymes.*" Our studies on the mechanism of action of OMPDC provide strong evidence that catalysis by this enzyme is not fundamentally different from less proficient catalysts, while highlighting important architectural elements that enable a peak level of performance. Many enzymes undergo substrate-induced protein conformational changes that trap their substrates in solvent occluded protein cages, but the conformational change induced by ligand binding to OMPDC is incredibly complex, as required to enable the development of 22 kcal/mol of stabilizing binding interactions with the phosphodianion and ribosyl substrate fragments of OMP. The binding energy from these fragments is utilized to activate OMPDC for catalysis of decarboxylation at the orotate fragment of OMP, through the creation of a tight, catalytically active, protein cage from the floppy, open, unliganded form of OMPDC. Such utilization of binding energy for ligand-driven conformational changes provides a general mechanism to obtain specificity in transition state binding. The rate enhancement that results from the binding of carbon acid substrates to enzymes is partly due to a reduction in the carbon acid pK_a that is associated with ligand binding. The binding of UMP to OMPDC results in an unusually large >12 unit decrease in the pK_a = 29 for abstraction of the C-6 substrate hydrogen, due to stabilization of an enzyme-bound vinyl carbanion, which is also an intermediate of OMPDC-catalyzed decarboxylation. The protein−ligand interactions operate to stabilize the vinyl carbanion at the enzyme active site compared to aqueous solution, rather than to stabilize the transition state for the concerted electrophilic displacement of CO_2 by H^+ that avoids formation of this reaction intermediate. There is evidence that OMPDC induces strain into the bound substrate. The interaction between the amide side chain of Gln-215 from the phosphodianion gripper loop and the hydroxymethylene side chain of Ser-154 from the pyrimidine umbrella of *Sc*OMPDC position the amide side chain to interact with the phosphodianion of OMP. There are no direct stabilizing interactions between dianion gripper protein side chains Gln-215, Tyr-217, and Arg-235 and the pyrimidine ring at the decarboxylation transition state. Rather these side chains function solely to hold OMPDC in the catalytically active closed conformation. The hydrophobic side chains that line the active site of OMPDC in the region of the departing CO_2 product may function to stabilize the decarboxylation transition state by providing hydrophobic solvation of this product.

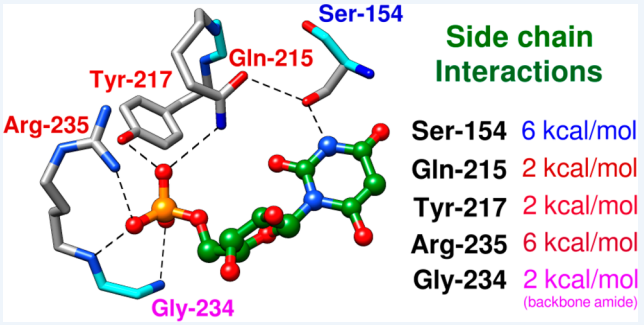

I. INTRODUCTION

Enzymes operate at different levels of performance;[1] and one of the challenges for mechanistic enzymologists is to define protein architectural elements that enable enzymes to perform at the highest level.[2] Amyes and Richard recognized this challenge, after spending years investigating the mechanism for nonenzymatic reactions.[3,4] The obvious target for study was the decarboxylation reaction catalyzed by orotidine 5′-monophosphate decarboxylase (OMPDC), because the 10^{23}-fold rate acceleration for this enzyme corresponds to an enormous 31 kcal/mol stabilization of the transition state for the chemically difficult decarboxylation of orotidine 5′-monophosphate (OMP) to give uridine 5′-monophosphate (UMP, Scheme 1) represented an extraordinary rate enhancement for a unimolecular reaction.[5]

High-resolution X-ray crystal structures of OMPDC resulted in a flurry of controversy and activity, because of their failure to lead to a consensus decarboxylation reaction mechanism.[6] This gave rise to provocative statements. For example, it was claimed that "*This proficient enzyme jolted many biochemists' assumptions about the catalytic potential of enzymes...*"[7] A second group claimed that "*the 10^{23} M^{-1} proficiency of ODC must arise from covalent catalysis, since only 10^{11} M^{-1} proficiency is possible by noncovalent binding,*"[8] even though there was no solid

Received: February 2, 2018
Published: March 29, 2018

DOI: 10.1021/acs.accounts.8b00059
Acc. Chem. Res. 2018, 51, 960–969

Scheme 1. OMDPC-Catalyzed Decarboxylation of OMP to form UMP

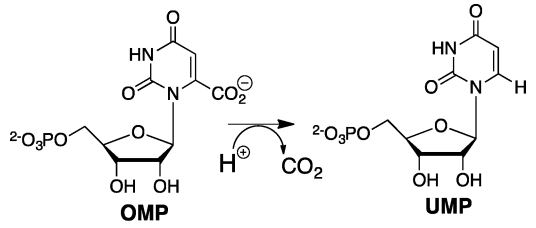

experimental evidence to support covalent catalysis by OMPDC. We eagerly joined in the quest to determine how OMPDC works, while viewing these statements with skepticism. In fact, the rate acceleration by OMPDC is only incrementally greater than that for other enzymes.[1] We have therefore embraced, and worked to build on, the extraordinary work of mechanistic enzymologists over the past 50 years, in defining the mechanism of action for OMPDC.

II. THE PAULING PRINCIPLE

Catalysis by OMPDC is due to stabilization of the decarboxylation transition state by interactions with the protein catalyst.[9,10] These must be 31 kcal/mol to account for the 10^{23}-fold rate acceleration. The falloff in the second-order rate constants for OMPDC-catalyzed decarboxylation observed upon the truncation of the phosphodianion and the ribosyl phosphate from the substrate OMP, provide intrinsic binding energies of 11.8 and 10.6 kcal/mol for these substrate fragments, and of 8.6 kcal/mol for the pyrimidine ring (Scheme 2).[11,12]

Scheme 2. Partitioning of the Transition State Binding Energy for Yeast OMPDC (*Sc*OMPDC)-Catalyzed Decarboxylation of OMP

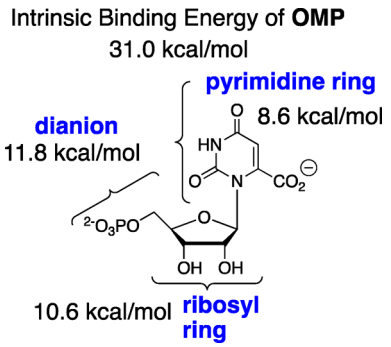

This pedantic division of the substrate intrinsic binding energy provides limited insight into reaction mechanism, but is the first step toward the more enlightening characterization of the specificity of these substrate fragments for binding to the transition state for OMPDC-catalyzed decarboxylation. For example, phosphite dianion shows barely detectable binding to free *Sc*OMPDC (K_d > 0.1 M). However, an analysis of strong phosphite dianion activation of *Sc*OMPDC-catalyzed decarboxylation of the truncated substrate 1-(β-D-erythrofuranosyl)-orotic acid (EO) gives $K_{act}^{‡}$ = 2.2 × 10^{-6} M for dianion binding to the transition state (eq 1, derived for Scheme 3), where $(k_{cat}/K_m)_0$ = 0.026 M^{-1} s^{-1} and $(k_{cat}/K_m)_{HPi}/K_d$ = 12 000 M^{-2} s^{-1} are the experimental rate constants for unactivated and phosphite dianion activated *Sc*OMPDC-catalyzed decarboxylation of EO.[13,14] These data show that 8 of the 12 kcal/mol intrinsic phosphodianion binding energy of OMP is recovered in HP_i, as *activation* of *Sc*OMPDC for catalysis of decarboxylation of EO. The remaining 4 kcal/mol of binding energy represents the largely entropic advantage of unimolecular enzyme-catalyzed decarboxylation of the whole substrate compared with the bimolecular reaction of the substrate pieces.[15]

Scheme 3. Kinetic Scheme That Describes the Activation of *Sc*OMPDC-Catalyzed Decarboxylation of EO and FEO by Phosphite Dianion (eq 1)

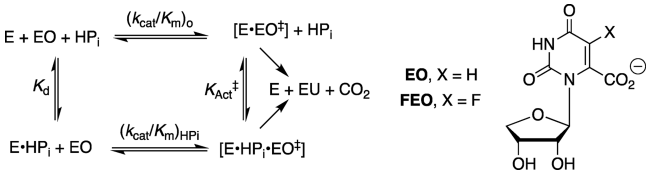

$$K_{act}^{‡} = \left(\frac{K_d(k_{cat}/K_m)_0}{(k_{cat}/K_m)_{HPi}}\right) \quad (1)$$

The activation of *Sc*OMPDC for catalysis of decarboxylation of EO observed for a wide range of dianions, with intrinsic dianion binding energies $\Delta G^{‡}$ shown in Chart 1, is consistent with a binding locus at *Sc*OMPDC where dianion binding energy is utilized to enhance catalysis at a distant pyrimidine binding locus.[14,16] *Sc*OMPDC also catalyzes decarboxylation of 1-(β-D-erythrofuranosyl)-5-fluoroorotate (FEO) and of 5-fluoroorotate (FO).[11] Each enzymatic reaction is activated by phosphite dianion (see Scheme 3), and a similar 5 kcal/mol stabilization of the respective reaction transition states by 1.0 M dianion is observed (Scheme 4).[11] The transition state for

Chart 1. Binding Energies $\Delta G^{‡}$ for Stabilization of the Transition State for *Sc*OMPDC-Catalyzed Decarboxylation of EO by Different Dianions, Calculated from the Dissociation Constants for Breakdown of Dianion Transition State Complexes[14,16]

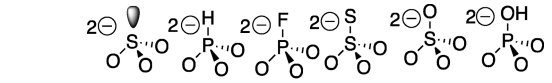

ΔG‡ kcal/mol	-8.3	-7.7	-6.7	-4.6	-4.5	-3.0

Scheme 4. Activation of *Sc*OMPDC-Catalyzed Decarboxylation, Where $\Delta G^{‡}$ is for Activator Binding to the Transition State for OMDC-Catalyzed Decarboxylation of a Truncated Substrates EO or FO (Scheme 3)

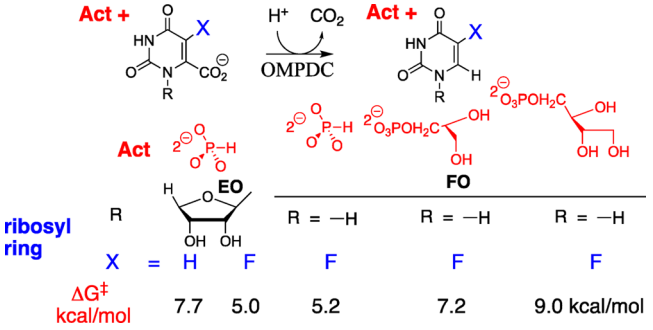

DOI: 10.1021/acs.accounts.8b00059
Acc. Chem. Res. 2018, 51, 960−969

*Sc*OMPDC-catalyzed decarboxylation of FO is stabilized by 5.2, 7.2, and 9.0 kcal/mol, respectively, by 1.0 M phosphite dianion, D-glycerol 3-phosphate and D-erythritol 4-phosphate, *so that binding interactions between both the substrate phosphodianion and the ribosyl hydroxyls are utilized to activate ScOMPDC for catalysis.*[11]

III. ENZYME-ACTIVATING CONFORMATIONAL CHANGES

Scheme 5 shows the model that rationalizes the activation of OMPDC for catalysis by interactions with dianions (Chart 1)

Scheme 5. Enzyme-Activating, Ligand Driven Conformational Change

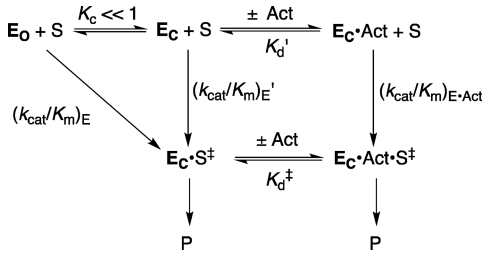

and ribosyl-type hydroxyl groups (Scheme 4).[10,17,18] OMPDC undergoes a large thermodynamically unfavorable ($K_C \ll 1$, Scheme 5) conformational change that transforms this enzyme from an inactive, floppy and disordered open form (E_O) to an active, tight structured substrate cage (E_C).[2,19,20] Activation of OMPDC and other enzymes results when ligand binding gives rise to an increase in the fraction of protein present as E_C.[21] Scheme 5 shows a substrate-induced fit that was referred to by Koshland, in another context, as an "induced-fit".[22] Koshland's induced fit model was criticized because it did not provide a rational for the evolution of enzymes that exist mainly as inactive E_O.[23] However, we expect that there should normally be a barrier to conversion of a loose, open, enzyme E_O to the tight, closed, caged complexe E_C, and have proposed that this represents the barriers to extrusion of protein bound waters to bulk solvent; and, to freezing motions at protein loops and catalytic side chains at the structured cage.[17]

X-ray Crystal Structures of E_O and E_C

Figure 1 (top structures) shows space filling representations of the unliganded and the 6-hydroxyuridine 5′-monophosphate (BMP) complex to OMPDC from yeast (*Sc*OMPDC). The solvent exposed active site of E_O lies between open phosphodianion (Pro-202 to Val-220) and pyrimidine gripper (Ala-151 to Thr-165) loops that are shaded blue. These loops close over BMP at E_C. The side chain of Arg-235 (shaded green) at the surface of *Sc*OMPDC forms an ion pair to the ligand phosphodianion. The R235A mutation of *Sc*OMPDC results in a 5.8 kcal/mol destabilization of the transition state for *Sc*OMPDC-catalyzed decarboxylation; and, 3.0 kcal/mol of this effect is "rescued" by guanidine cation, which mimics the excised side chain.[24]

The middle structures from Figure 1 show the complex between *Sc*OMPDC and 6-aza uridine 5′-monophosphate (azaUMP) on the right, and the structure of unliganded *Sc*OMPDC on the left, in which a hypothetical 6-aza uridine 5′-monophosphate (azaUMP) ligand has been inserted at the position determined for the *Sc*OMPDC·azaUMP complex.[25] The middle structures from Figure 1 show that ligand binding

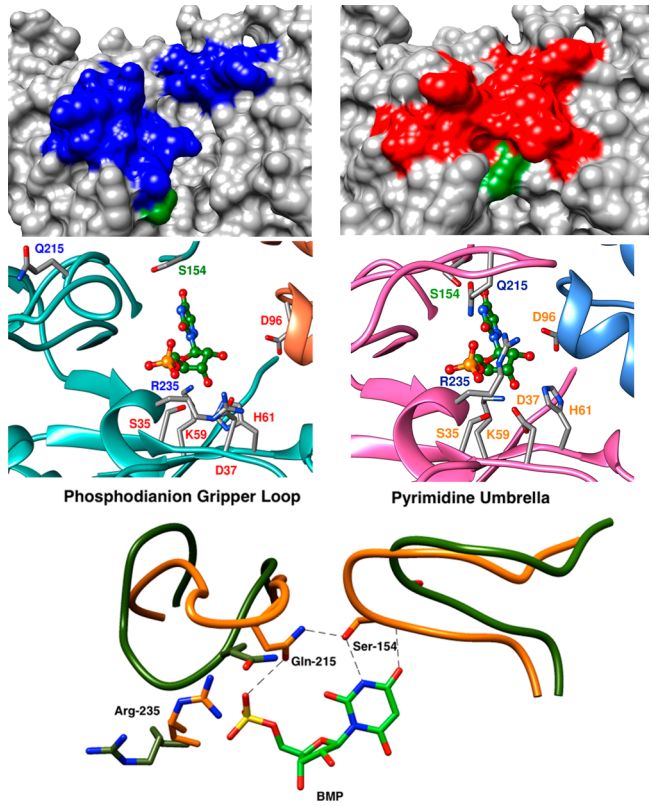

Figure 1. Representations of the open (E_O) and the closed (E_C) forms of *Sc*OMPDC. Top: Space filling models of open unliganded *Sc*OMPDC (left, PDB entry 1DQW) and the caged complex to BMP (right, 1DQX). The Arg-235 guanidine side chain is shaded green. Middle: Representations of the open (E_O, left, 3GDK) and closed (E_C, right, 3GDL) forms of *Sc*OMPDC.[25] The azaUMP ligand is placed at E_O at the position determined for E_C. Bottom: Image that superimposes partial X-ray crystal structures of the OMPDC·BMP complex (PDB entry 1DQX) over the structure for unliganded *Sc*OMPDC (1DQW). The movement of the phosphodianion gripper loop (Pro-202 to Val-220) toward the pyrimidine umbrella (Ala-151 to Thr-165) is shown. Reprinted with permission from ref 39. Copyright 2013 American Chemical Society.

is driven by the development of stabilizing interactions between the phosphodianion and the side chains of Arg-235 and Gln-215, and between the ribosyl hydroxyls and the side chains of Asp-96, His-61, Asp-37, and Lys-59. All of these interactions act to stabilize E_C relative to E_O, and activate *Sc*OMPDC for catalysis of decarboxylation of truncated substrates (Scheme 4).

The bottom structures from Figure 1 show interactions, that arise from the ligand driven conformational change, of the amide side chain of Gln-215 (phosphodianion gripper loop) with the phosphodianion and with the hydroxymethylene side chain of Ser-154 (pyrimidine umbrella). The role of this interloop interaction in catalysis was probed by determining the effects of S154A, Q215A and S154A/Q215A mutations on $\Delta G^{\ddagger}$ for *Sc*OMPDC-catalyzed decarboxylation of OMP (Scheme 6).[26] The Q215A mutation results in 0.5 and 1.8 kcal/mol increases, respectively, in the barrier for *Sc*OMPDC-catalyzed decarboxylation of EO and OMP that are consistent with an interaction between the amide side chain and the phosphodianion of OMP. The Q215A mutation of wild type *Sc*OMPDC results in a 1.8 kcal/mol destabilization of the decarboxylation transition state, while the same mutation at the S154A mutant results in only a 0.3 kcal/mol change,[27] because the interloop

DOI: 10.1021/acs.accounts.8b00059
Acc. Chem. Res. 2018, 51, 960−969

Scheme 6. Effect S154A and Q215A Mutations on the Activation Barrier $G^{‡}$ (k_{cat}/K_m) for Wild Type *Sc*OMPDC-Catalyzed Decarboxylation of OMP

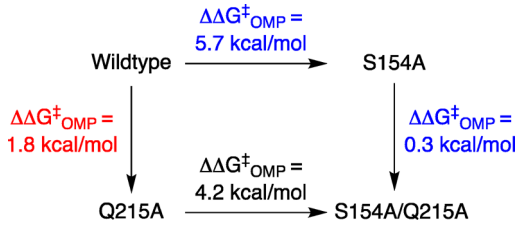

interaction between the side chains of Ser-154 and Gln-215 wild type *Sc*OMPDC (Figure 1, bottom) is required to hold the amide side chain in a position to interact with the substrate phosphodianion.

Steric Effects on Cage Formation

Small changes in substrate bulk result in dramatic changes in the barrier to *Sc*OMPDC-catalyzed decarboxylation (Chart 2). For example, adding a $-CH_2OH$ group to EO or an $-OH$ group to phosphite dianion results in 8.3 and 4.7 kcal/mol increases, respectively, in the barrier to the dianion-activated decarboxylation; the combined effect of these two substitutions is ca. 13 kcal/mol.[13,28] These data define an estimated rate constant of 3.4×10^{-6} M^{-1} s^{-1} for phosphate dianion activation of *Sc*OMPDC-catalyzed decarboxylation orotidine, which was too small to detect by experiment.[29] Addition of a $-CH_2OH$ group to EO results in a 3.0 kcal/mol increase in the barrier to unactivated *Sc*OMPDC-catalyzed decarboxylation, while addition of a $-PO_3^{-2}$ group of orotidine results in a 14.7 kcal/mol reduction in the barrier to decarboxylation that is even larger than the 11.7 kcal/mol effect of addition of a $-CH_2OPO_3^{2}$ group to EO (Chart 2).[13,28]

No significant electronic effects are expected by groups distant from the reacting pyrimidine ring; and, only small steric effects are expected by these groups for ligand binding to the open enzyme (E_O). The results from Chart 2 are consistent with a reaction that proceeds through an extraordinarily crowded and reactive *preorganized* closed protein cage E_C, where small disruptions of the cage structure result in large increases in the activation barrier for *Sc*OMPDC-catalyzed decarboxylation.[30,31] The 3.0 kcal/mol larger barrier for unactivated *Sc*OMPDC-catalyzed decarboxylation of orotidine compared to EO is a surprising $-CH_2OH$ substituent effect, because the larger $-CH_2OPO_3^{2-}$ group results in an 11.9 *reduction* in the reaction barrier. Apparently, the binding energy for OMP, orotidine, and EO is utilized for the stabilization of a similar caged protein complexes E_C, whose stability is perturbed in some way by the $-OH$ group of orotidine.

IV. REACTION MECHANISM

The simplest mechanism for OMPDC, direct decarboxylation of OMP to form a vinyl carbanion reaction intermediate, was viewed with skepticism,[32,33] in part because of the failure to detect OMPDC-catalyzed exchange of deuterium from solvent D_2O with the C-6 H of UMP to form *d*-UMP (Scheme 7).[34] While the cut of Occam's razor is sometimes ragged, we suspected that the experiments to detect the OMPDC-catalyzed deuterium exchange reaction were inconclusive, due to the use of a low concentration of OMPDC, a too-short reaction time, and a less than optimal pD.[34] This skepticism led to experiments which detected (a) *Sc*OMPDC-catalyzed (0.10−0.30 mM enzyme) exchange for deuterium of the C-6 protons of uridine 5′-monophosphate (UMP) using ^{1}H NMR spectroscopy (Scheme 7);[35,36] (b) the faster *Sc*OMPDC deuterium exchange reaction of 5-fluorouridine 5′-monophosphate (F-UMP); and (c) a sharp increase in the reaction velocity as the pD was increased from 7.0 to 9.4.

The following observations provide strong evidence that the OMPDC-catalyzed decarboxylation and deuterium exchange reactions proceed through a common vinyl carbanion intermediate (Scheme 7).

Chart 2. Rate Constants and Changes in Activation Barriers $\Delta\Delta G^{‡}$ for *Sc*OMPDC-Catalyzed Decarboxylation of the Substrate Pieces (Top Row) Or the Whole Substrate OMP (Bottom Row)[a]

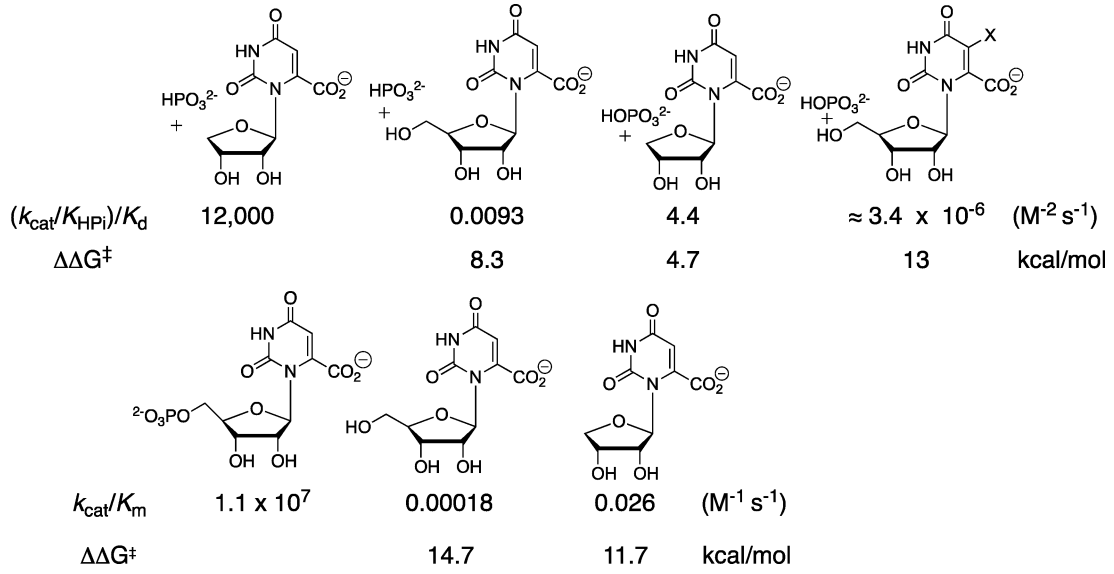

[a] $\Delta\Delta G^{‡}$ is the effect of substitutions on the stability of the transition state for either dianion activated *Sc*OMPDC-catalyzed decarboxylation of EO or direct decarboxylation of OMP.

DOI: 10.1021/acs.accounts.8b00059
Acc. Chem. Res. 2018, 51, 960−969

Scheme 7. Decarboxylation and Deuterium Exchange Reactions Catalyzed by *Sc*OMPDC

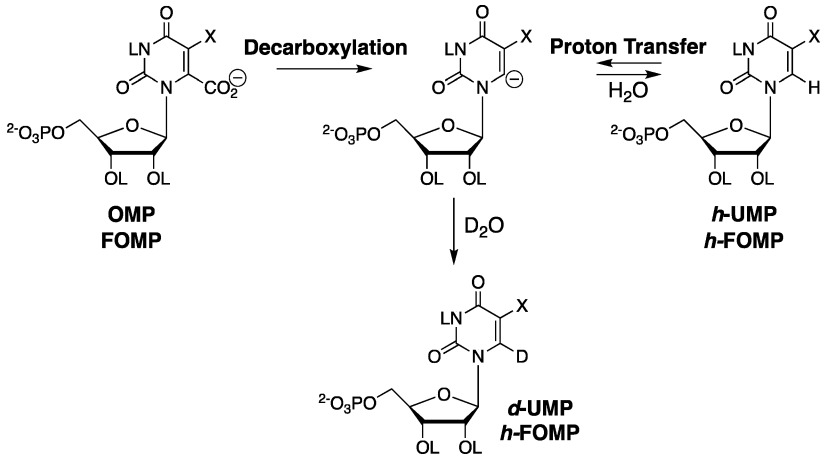

Scheme 8. Phosphite Dianion Activation of the *Sc*OMPDC-Catalyzed Deuterium Exchange Reaction of *h*-FEU

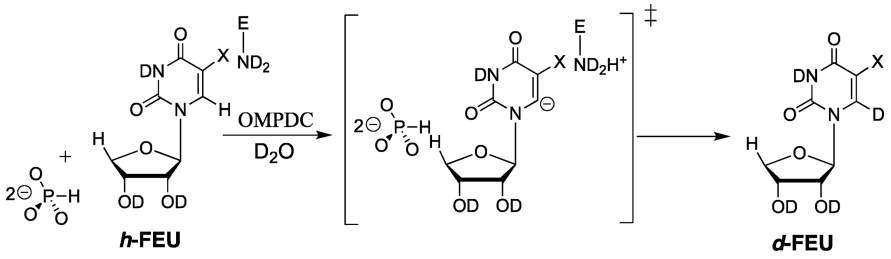

(1) The electron-withdrawing C-5 F pyrimidine substituent shows substantial 4.8 and 3.2 kcal/mol stabilizing interactions, respectively, with the transition states for the wild type *Sc*OMPDC-catalyzed deuterium exchange reaction of FUMP and the Q215A/R235A mutant *Sc*OMPDC-catalyzed decarboxylation reaction of OMP,[35,37] where chemistry is strongly rate-determining for the decarboxylation reaction. This is consistent with a large buildup of negative charge at C-6 for the two transition states.

(2) The transition states for *Sc*OMPDC-catalyzed decarboxylation reactions of EO and FEO (Scheme 3) and for the *Sc*OMPDC-catalyzed deuterium exchange reaction of FEU (Scheme 8) are stabilized by 7.8, 5.0, and 5.8 kcal/mol, respectively, by the binding of 1.0 M phosphite dianion.[13,28,38] The similar dianion activation of *Sc*OMPDC-catalyzed decarboxylation and deuterium exchange reactions of FEO and FEU, respectively, provides strong evidence that activation is due to the stabilization of a common vinyl carbanion reaction intermediate.

(3) The guanidine side chain of Arg-235 forms an ion pair with the C-5′ phosphodianion of substrates bound to *Sc*OMPDC (Figure 1, top panel). The R235A mutation of *Sc*OMPDC results in a 5.6 kcal/mol destabilization of the transition states for enzyme-catalyzed decarboxylation of OMP, and a 7.2 kcal/mol destabilization of the transition state for enzyme-catalyzed exchange of the C-6 proton of FUMP (Scheme 9).[39] Guanidine cation, an analog of the arginine side chain, likewise shows a high efficiency for rescue of the lost activity for *Sc*OMPDC-catalyzed decarboxylation and deuterium exchange reactions that result from an R235A mutation.[24,39]

Scheme 9. Stabilizing Interaction between the R235 Side Chain and Transition States for *Sc*OMPDC-Catalyzed Reactions

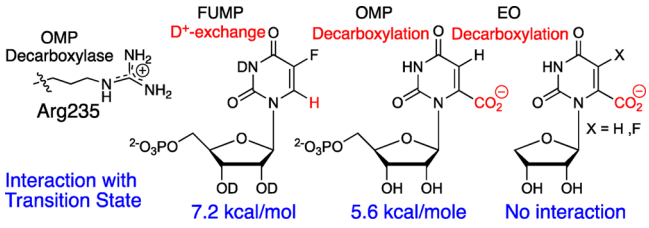

Stepwise or Concerted Decarboxylation?

Loss of CO_2 and the addition of a proton to carbon-6 of OMP may proceed by a stepwise (Scheme 7) or a concerted reaction mechanism, where there is electrophilic push to the loss of CO_2.[33] The 50:50 yield of *h*-UMP and *d*-UMP products determined for *Sc*OMPDC-catalyzed decarboxylation of OMP in 50:50 (v/v) H_2O/D_2O (eq 2 for Scheme 10) gives a PIE = 1.0 for the product deuterium isotope effect, where the PIE is equal to the 1°DKIE on the barrier to formation of the decarboxylation transition state from solvent, OMPDC and OMP.[40] This result provides strong evidence for stepwise decarboxylation, because the increase in bonding to the transferred hydron that occurs on proceeding to the transition state for a concerted reaction mechanism requires the observation of a 1°DKIE of >1.[41,42]

$$1°\mathrm{DKIE} = \mathrm{PDIE} = \frac{f_D[P_H]}{f_H[P_D]} = 1.0 \qquad (2)$$

We proposed that the statistical yield of *h*-UMP and *d*-UMP is enforced because the vinyl carbanion intermediate cannot

DOI: 10.1021/acs.accounts.8b00059
Acc. Chem. Res. 2018, 51, 960−969

Scheme 10. Decarboxylation of OMP in 50:50 (v/v) H_2O/D_2O To Form *h*-UMP and *d*-UMP

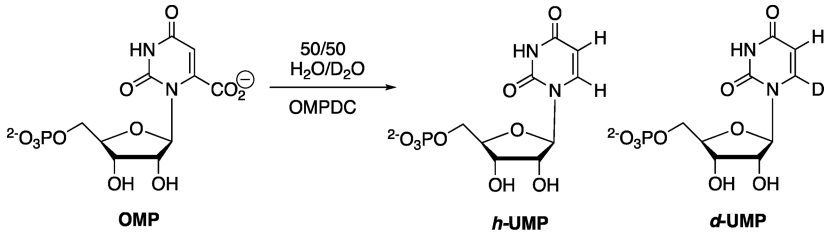

Scheme 11. Mechanism for *Sc*OMPDC-Catalyzed Decarboxylation, Which Shows Partitioning of the Vinyl Carbanion Intermediate between Direct Protonation (k_{-p}), and C−N Bond Rotation of the $-CH_2-NL_3^+$ Group (k_{rot}) Followed by Transfer of a Second Hydron (k'_{-p})

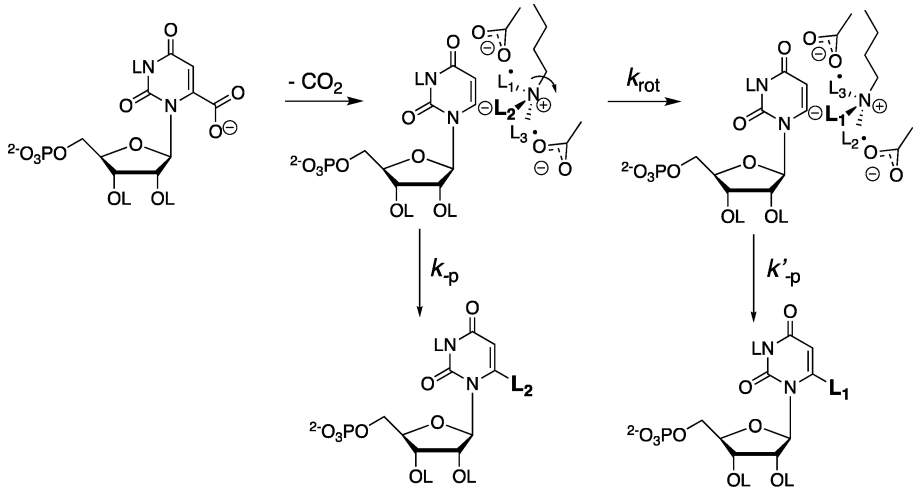

Scheme 12. Reversible *Sc*OMPDC-Catalyzed Deprotonation of UMP or FUMP Followed C−N Bond Rotation of the $-CH_2-NL_3^+$ Group That Leads to Exchange of the C-6 Hydrogen for Deuterium

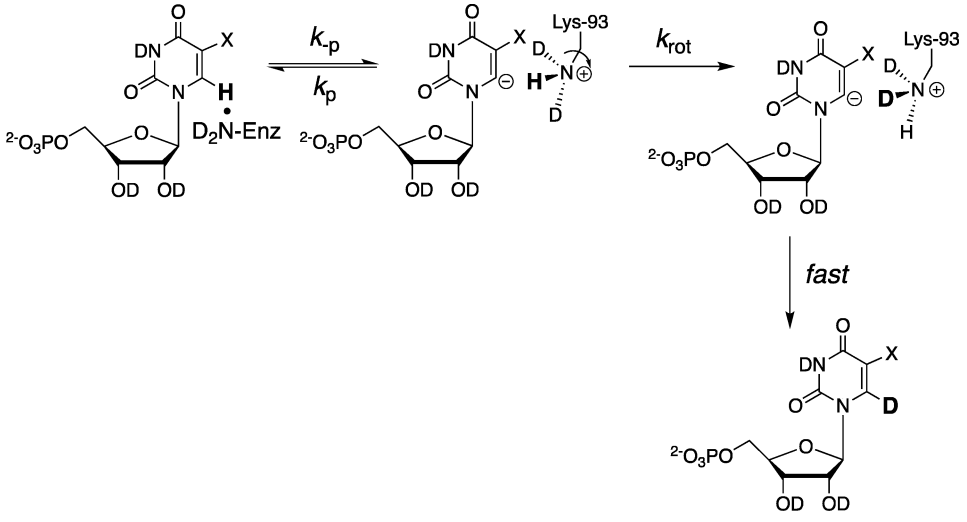

select between protonation by −H and −D from the $-CH_2-NL_3^+$ group of Lys-93 [the catalytic acid], due to restriction of C−N bond rotation by hydrogen bonds to Asp-91 and Asp-96 carboxylate groups, so that $k_{rot} \ll k_p$ (Scheme 11).[20] A rate constant of $k_{rot} \approx 10^4$ s^{-1} was estimated from the approximate value of $k_{rot} = 10^{11}$ s^{-1} for unhindered bond rotation,[43] and barriers of ca. 5 kcal/mol to cleavage of each of the hydrogen bonds.[41] Values of PIE = 1.0, also consistent with $k_{rot} \ll k_p$ (Scheme 11), were determined for *Sc*OMPDC-catalyzed decarboxylation of OMP and FOMP catalyzed by R235A, Y217A, Q215A, S154A, and S154A/Q215A mutant enzymes.[41]

$(K_{eq})_{enz}$ for Deprotonation of Enzyme-Bound UMP and FUMP

The equilibrium constants $(K_{eq})_{enz} = (k_{-p}/k_p)$ for formation of vinyl carbanions generated by deprotonation of UMP or FUMP at the active site of *Sc*OMPDC were estimated from the values of $(k_{ex})_{max}$ for *Sc*OMPDC-catalyzed deuterium exchange (eq 3, $k_{rot} \ll k_p$, Scheme 12), and using the above value of $k_{rot} \approx 10^4$ s^{-1} (eq 4). The values of $(k_{ex})_{max} = 1.2 \times 10^{-5}$ and 0.041 s^{-1}

DOI: 10.1021/acs.accounts.8b00059
Acc. Chem. Res. 2018, 51, 960−969

that were determined for deuterium exchange into enzyme-bound UMP and FUMP, respectively, were substituted into eq 4 to give equilibrium constants for proton transfer of $(K_{eq})_{enz}$ = 1.2×10^{-9} and 4.1×10^{-6}, respectively. By comparison, the equilibrium constants for proton transfer from C-6 of UMP and F-UMP to a primary amine base of pK_{RNH_3} = 7 *in water* were estimated to be $(K_{eq})_{aq} = 2 \times 10^{-22}$ and 8×10^{-19}, respectively, for UMP and FUMP. We concluded that the binding of UMP or FUMP to *Sc*OMPDC results in a ca. 17 kcal/mol stabilization of the enzyme bound vinyl carbanions by interaction with the protein catalyst, which corresponds to a 12 unit decrease in the pK_a for the enzyme-bound carbon acid. This is a substantial fraction of the total 31 kcal/mol stabilization of the transition state for *Sc*OMPDC-catalyzed decarboxylation, but falls short of accounting for the whole rate acceleration.[35]

$$(k_{ex})_{max} = \left(\frac{k_{-p}}{k_p}\right)k_{rot} = (K_{eq})_{enz}k_{rot} \quad (3)$$

$$(K_{eq})_{enz} = \left(\frac{(k_{ex})_{max}}{k_{rot}}\right) \quad (4)$$

V. UTILIZATION OF INTRINSIC DIANION BINDING ENERGY

We examined the activation of *Sc*OMPDC from protein-dianion interactions by preparing all combinations of single, double, and triple mutations of the protein side chains that interact with the phosphodianion [Figure 2; Arg-235 (R235A), Gln-215 (Q215A), and Tyr-217 (Y217F)], and characterizing their effect on enzyme activity.[21] The results of these studies show the following.

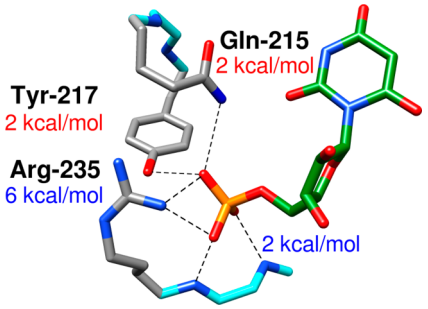

Figure 2. Contribution of *Sc*OMPDC gripper side chains to the intrinsic phosphodianion binding energy (eq 5) utilized for stabilization of the transition state for OMPDC-catalyzed decarboxylation.[12]

$$(\Delta G^{\ddagger})_{Pi} = -RT \ln\left(\frac{(k_{cat}/K_m)_{OMP}}{(k_{cat}/K_m)_{EO}}\right) \quad (5)$$

(1) The effect of single Q215A, Y217F, and R235A mutations on the intrinsic dianion binding energy $(\Delta G^{\ddagger})_{Pi}$ was calculated from their effect on the ratio of the second-order rate constants for *Sc*OMPDC-catalyzed reactions of whole and truncated substrates (eq 5). Figure 2 shows that these interactions account for (6 + 2 + 2) = 10 of the total 12 kcal/mol dianion binding energy. The remaining 2 kcal/mol of the dianion binding was attributed to hydrogen bonds to the backbone amides of Gly-234 and Arg-235.

(2) The mutant cube (Figure 3) summarizes the effects of mutations of Q215, Y217, and R235 on $(\Delta G^{\ddagger})_{OMP}$ for *Sc*OMPDC-catalyzed decarboxylation of OMP. This cube shows that the effect of a point mutation of residue X on $(\Delta\Delta G_X)_{OMP}$ is approximately the same when the mutation is carried out at wild type *Sc*OMPDC, singly mutated or doubly mutated forms of *Sc*OMPDC.[21] We concluded that mutations of these phosphodianion gripper side chains do not severely affect the functioning of the remaining side chains, and that there are only small interactions between the individual side chains.

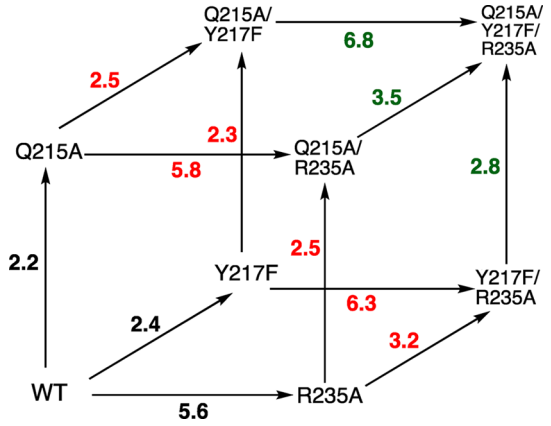

Figure 3. Triple mutant cube that summarizes the effects $(\Delta\Delta G^{\ddagger})_{OMP}$, in kcal/mol, of single amino acid mutations on $(\Delta G^{\ddagger})_{OMP}$ for the decarboxylation of OMP catalyzed by wild type *Sc*OMPDC (black values), by single mutants of *Sc*OMPDC (red values) and by double mutants of *Sc*OMPDC (green values).

(3) The Q215A, Y217F, and R235A (Scheme 9) mutations result in ≤2.4-fold decreases in k_{cat}/K_m for decarboxylation of (EO), while the Q215A/Y217F/R235A triple mutation results in only a 9-fold decrease in this kinetic parameter. Essentially the entire effect of these mutations is expressed as a decrease in the third-order rate constant for activation of the decarboxylation of EO by phosphite dianion, and this falloff in activity was so sharp that no dianion activation was detected for the reactions catalyzed by the Q215A/R235A, Y217F/R235A, and Q215A/Y217F/R235A mutants.[27] These results show that the dianion binding interactions with Gln-215, Tyr-217, and Arg-235 serve the exclusive function of activating OMPDC for catalysis at the pyrimidine binding site.

(4) There is a striking linear logarithmic correlation, with slope of 1.0, between the second and third order rate constants $(k_{cat}/K_m)_{OMP}$ and $k_{cat}/K_{HPi}K_{EO}$, respectively, for *Sc*OMPDC-catalyzed decarboxylation of OMP and for dianion activation of OMPDC-catalyzed decarboxylation of EO (Scheme 13).[21] This correlation shows that these two OMPDC-catalyzed reactions proceed through similar transition states that show similar interactions with dianion gripper side chains. The results are simply rationalized by a model in which phosphodianion binding interactions serve the sole function of locking *Sc*OMPDC into a reactive closed conformation (Scheme 5), so that these dianions are essentially spectators at the transition states for OMPDC-catalyzed decarboxylation.[21]

DOI: 10.1021/acs.accounts.8b00059
Acc. Chem. Res. 2018, 51, 960−969

Scheme 13. OMPDC-Catalyzed Reactions of the Whole Substrate OMP and the Pieces EO + HP_i

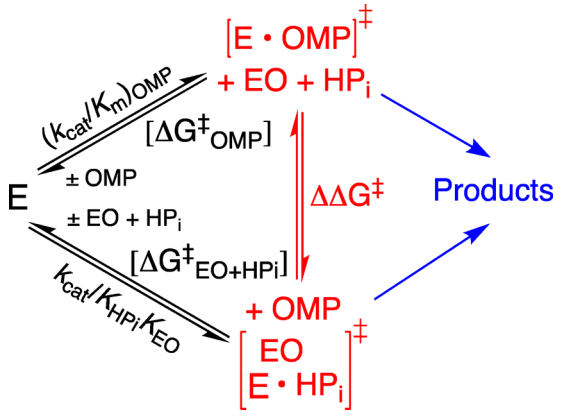

VI. OTHER ISSUES

Structural Heterogeneity of Dianion Gripper Loops

OMPDCs from different organisms show an overall high degree of catalytic structural homology, except for their phosphate gripper loops.[44] The loops for OMPDC from yeast (*Sc*OMPDC) and from *Escherichia coli* (*Ec*OMPDC) both extend 19 residues, from Pro-202 to Val-220 for *Sc*OMPDC[20] (Figure 1), and from Pro-189 to Pro-207 for EcOMPDC,[45,46] while the corresponding loop of OMPDC from the thermophile *Methanothermobacter thermautotrophicus* (*Mt*OMPDC) extends only 9 residues, from Pro-180 to Asp-188 (Figure 1).[47] Each enzyme shows strong activation for catalysis of decarboxylation of EO by the binding of phosphite dianion. The activation parameters $\Delta H^{\ddagger}$ and $\Delta S^{\ddagger}$ determined for k_{cat} for decarboxylation of OMP are 3.6 kcal/mol and 10 cal/K/mol more positive, respectively, for *Mt*OMPDC than for *Sc*OMPDC.[44] This shows that *Sc*OMPDC, which functions at relatively low temperatures, obtains the benefits of enthalpic transition state stabilization available from extensive loop−substrate interactions. By contrast, *Mt*OMPDC functions at higher temperatures and has sacrificed enthalpic transition state stabilization from a large loop, for a smaller loop that shows a reduced entropic requirement for immobilization at the protein.[44]

Ground-State Effects

There is evidence that protein−ligand interactions introduce strain into the bound substrate, that is relieved at the decarboxylation transition state.[47] (1) The binding of OMP to inactive mutants of OMPDC results in a ca. 40° movement of the carboxylate group at C-6 of OMP out of the plane of the pyrimidine ring.[48] (2) The results from studies on the effect of a D70N mutation of *Mt*OMPDC on the kinetic parameters for enzyme-catalyzed decarboxylation and deuterium exchange reactions are consistent with modest destabilization of the Michaelis complex by interactions between the substrate carboxylate and the carboxylate from Asp-70 of *Mt*OMPDC.[25]

Large rate enhancements for decarboxylation are observed upon transfer of substrates, such as 1-methylorotate, from water to organic solvents.[49] This has been attributed to the creation of electrostatic stress at the carboxylate in the organic solvent, that is relieved at the decarboxylation transition state. The pyrimidine ring of FUMP bound to *Sc*OMPDC is "sandwiched" between the hydrophobic side chains of Pro-202 and Ile-318′ of the second subunit, while the fluorine of FUMP projects into a hydrophobic pocket lined by the side chains of Leu-150, Leu-153, and Ile-183 at *Sc*OMPDC.[35] It is not clear that these hydrophobic side-chains create electrostatic stress at OMP; and, we note that the substrate carboxylate lies close to the cationic side chain of Lys-93 (Scheme 12), so that the binding energy of OMP is ca. 3 kcal/mol larger than for UMP.[50] We have proposed that the late transition state for *Sc*OMPDC-catalyzed decarboxylation of OMP is stabilized by the development of stabilizing interactions between the departing CO_2 and these hydrophobic protein side chains.[35]

VII. SUMMARY AND CONCLUSIONS

The controversy about the origin of the rate acceleration for OMPDC was partly due to the lack of protocol to evaluate the 31 kcal/mol intrinsic substrate binding energy.[12] We have shown that interactions between *Sc*OMPDC and the substrate ribosyl ring and phosphodianion are responsible for ca. 22 kcal/mol of this binding energy (Scheme 2). These interactions activate *Sc*OMPDC for catalysis of decarboxylation, where the activation is accomplished through the utilization of substrate binding energy to drive an extensive change in protein conformation, from an open and loose structure that shows relatively weak interactions with the substrate, to a tight protein cage that shows strong interactions with the transition state. The utilization of binding interactions for the creation of tight and catalytically active protein cages from floppy open forms is a widespread phenomenon, that provides a general and underappreciated mechanism to obtain specificity in transition state binding.[10,17]

The correlation between the magnitude of rate enhancements for enzymes that catalyze deprotonation of carbon, and the complexity of conformational changes of the open enzymes that trap their substrates in a protein cage,[2] extends to *Sc*OMPDC-catalyzed decarboxylation and deuterium exchange reactions. These large rate accelerations are enabled by the expansive protein conformational change illustrated in Figure 1, which places the pyrimidine ring of OMP in a structured protein cage, where the barrier to decarboxylation is lower than in water. The mechanism for the reduction in activation barrier has been modeled in computational studies,[47,51,52] but is still not entirely understood and will be the focus of our future work on OMPDC. Finally, we emphasize that this Account does not do justice to the complexity of the ligand-driven conformational change, in part because a full description of this change in protein structure is beyond the capabilities of the simple chemists in our group. We are not so simple as to fail to grasp the tremendous potential for protein engineers to contribute to our understanding of the mechanisms for protein catalysis, through modeling related conformational changes in designing catalytically active proteins.

AUTHOR INFORMATION

Corresponding Author

*E-mail: jrichard@buffalo.edu.

ORCID

John P. Richard: 0000-0002-0440-2387
Archie C. Reyes: 0000-0001-9955-393X

Notes

The authors declare no competing financial interest.

DOI: 10.1021/acs.accounts.8b00059
Acc. Chem. Res. 2018, 51, 960−969

Biographies

John P. Richard received a B.S. degree in biochemistry and his Ph.D. degree in chemistry (1979) from The Ohio State University. He is currently UB Distinguished Professor of Chemistry at the University at Buffalo, SUNY.

Tina L. Amyes received B.A. and M.A. degrees in natural sciences and her Ph.D. degree in chemistry (1986) from the University of Cambridge (England). She is currently Team Science Grant Coordinator at the Roswell Park Cancer Institute.

Archie C. Reyes received his B.S. degree in chemistry (2006) and M.S. degree in biochemistry (2010) from the University of the Philippines Los Baños, and his Ph.D. degree in Chemistry (2017) from the University at Buffalo SUNY, where he is currently employed as a Research Scientist.

■ ACKNOWLEDGMENTS

This work was supported by grants from the United States National Institutes of Health: GM116921 and GM039754. We thank Prof. John Gerlt for insightful observations during our collaborative work on the mechanism of action of OMPDC.

■ REFERENCES

(1) Wolfenden, R.; Snider, M. J. The Depth of Chemical Time and the Power of Enzymes as Catalysts. *Acc. Chem. Res.* **2001**, *34*, 938−945.
(2) Richard, J. P.; Amyes, T. L.; Goryanova, B.; Zhai, X. Enzyme architecture: on the importance of being in a protein cage. *Curr. Opin. Chem. Biol.* **2014**, *21*, 1−10.
(3) Morrow, J. R.; Amyes, T. L.; Richard, J. P. Phosphate Binding Energy and Catalysis by Small and Large Molecules. *Acc. Chem. Res.* **2008**, *41*, 539−548.
(4) Richard, J. P.; Amyes, T. L.; Toteva, M. M. Formation and Stability of Carbocations and Carbanions in Water and Intrinsic Barriers to Their Reactions. *Acc. Chem. Res.* **2001**, *34*, 981−988.
(5) Radzicka, A.; Wolfenden, R. A proficient enzyme. *Science* **1995**, *267*, 90−93.
(6) Houk, K. N.; Lee, J. K.; Tantillo, D. J.; Bahmanyar, S.; Hietbrink, B. N. Crystal structures of orotidine monophosphate decarboxylase: does the structure reveal the mechanism of nature's most proficient enzyme? *ChemBioChem* **2001**, *2*, 113−118.
(7) Callahan, B. P.; Miller, B. G. OMP decarboxylase - An enigma persists. *Bioorg. Chem.* **2007**, *35*, 465−469.
(8) Zhang, X.; Houk, K. N. Why enzymes are proficient catalysts: beyond the Pauling paradigm. *Acc. Chem. Res.* **2005**, *38*, 379−385.
(9) Pauling, L. The nature of forces between large molecules of biological interest. *Nature* **1948**, *161*, 707−709.
(10) Amyes, T. L.; Richard, J. P. Specificity in transition state binding: The Pauling model revisited. *Biochemistry* **2013**, *52*, 2021−2035.
(11) Reyes, A. C.; Amyes, T. L.; Richard, J. Enzyme Architecture: Erection of Active Orotidine 5′-Monophosphate Decarboxylase by Substrate-Induced Conformational Changes. *J. Am. Chem. Soc.* **2017**, *139*, 16048−16051.
(12) Jencks, W. P. Binding energy, specificity, and enzymic catalysis: the Circe effect. *Adv. Enzymol. Relat. Areas Mol. Biol.* **2006**, *43*, 219−410.
(13) Amyes, T. L.; Richard, J. P.; Tait, J. J. Activation of orotidine 5′-monophosphate decarboxylase by phosphite dianion: The whole substrate is the sum of two parts. *J. Am. Chem. Soc.* **2005**, *127*, 15708−15709.
(14) Reyes, A. C.; Zhai, X.; Morgan, K. T.; Reinhardt, C. J.; Amyes, T. L.; Richard, J. P. The Activating Oxydianion Binding Domain for Enzyme-Catalyzed Proton Transfer, Hydride Transfer and Decarboxylation: Specificity and Enzyme Architecture. *J. Am. Chem. Soc.* **2015**, *137*, 1372−1382.
(15) Jencks, W. P. On the attribution and additivity of binding energies. *Proc. Natl. Acad. Sci. U. S. A.* **1981**, *78*, 4046−4050.
(16) Spong, K.; Amyes, T. L.; Richard, J. P. Enzyme Architecture: The Activating Oxydianion Binding Domain for Orotidine 5′-Monophophate Decarboxylase. *J. Am. Chem. Soc.* **2013**, *135*, 18343−18346.
(17) Amyes, T. L.; Malabanan, M. M.; Zhai, X.; Reyes, A. C.; Richard, J. P. Enzyme activation through the utilization of intrinsic dianion binding energy. *Protein Eng., Des. Sel.* **2017**, *30*, 159−168.
(18) Go, M. K.; Amyes, T. L.; Richard, J. P. Hydron Transfer Catalyzed by Triosephosphate Isomerase. Products of the Direct and Phosphite-Activated Isomerization of [1-^{13}C]-Glycolaldehyde in D_2O. *Biochemistry* **2009**, *48*, 5769−5778.
(19) Malabanan, M. M.; Amyes, T. L.; Richard, J. P. A role for flexible loops in enzyme catalysis. *Curr. Opin. Struct. Biol.* **2010**, *20*, 702−710.
(20) Miller, B. G.; Hassell, A. M.; Wolfenden, R.; Milburn, M. V.; Short, S. A. Anatomy of a proficient enzyme: the structure of orotidine 5′-monophosphate decarboxylase in the presence and absence of a potential transition state analog. *Proc. Natl. Acad. Sci. U. S. A.* **2000**, *97*, 2011−2016.
(21) Goldman, L. M.; Amyes, T. L.; Goryanova, B.; Gerlt, J. A.; Richard, J. P. Enzyme Architecture: Deconstruction of the Enzyme-Activating Phosphodianion Interactions of Orotidine 5′-Monophosphate Decarboxylase. *J. Am. Chem. Soc.* **2014**, *136*, 10156−10165.
(22) Koshland, D. E., Jr. Application of a Theory of Enzyme Specificity to Protein Synthesis. *Proc. Natl. Acad. Sci. U. S. A.* **1958**, *44*, 98−104.
(23) Herschlag, D. The role of induced fit and conformational changes of enzymes in specificity and catalysis. *Bioorg. Chem.* **1988**, *16*, 62−96.
(24) Barnett, S. A.; Amyes, T. L.; McKay Wood, B.; Gerlt, J. A.; Richard, J. P. Activation of R235A Mutant Orotidine 5′-Monophosphate Decarboxylase by the Guanidinium Cation: Effective Molarity of the Cationic Side Chain of Arg-235. *Biochemistry* **2010**, *49*, 824−826.
(25) Chan, K. K.; Wood, B. M.; Fedorov, A. A.; Fedorov, E. V.; Imker, H. J.; Amyes, T. L.; Richard, J. P.; Almo, S. C.; Gerlt, J. A. Mechanism of the Orotidine 5′-Monophosphate Decarboxylase-Catalyzed Reaction: Evidence for Substrate Destabilization. *Biochemistry* **2009**, *48*, 5518−5531.
(26) Barnett, S. A.; Amyes, T. L.; Wood, B. M.; Gerlt, J. A.; Richard, J. P. Dissecting the Total Transition State Stabilization Provided by Amino Acid Side Chains at Orotidine 5′-Monophosphate Decarboxylase: A Two-Part Substrate Approach. *Biochemistry* **2008**, *47*, 7785−7787.
(27) Amyes, T. L.; Ming, S. A.; Goldman, L. M.; Wood, B. M.; Desai, B. J.; Gerlt, J. A.; Richard, J. P. Orotidine 5′-monophosphate decarboxylase: Transition state stabilization from remote protein-phosphodianion interactions. *Biochemistry* **2012**, *51*, 4630−4632.
(28) Goryanova, B.; Spong, K.; Amyes, T. L.; Richard, J. P. Catalysis by Orotidine 5′-Monophosphate Decarboxylase: Effect of 5-Fluoro and 4′-Substituents on the Decarboxylation of Two-Part Substrates. *Biochemistry* **2013**, *52*, 537−546.
(29) Sievers, A.; Wolfenden, R. The effective molarity of the substrate phosphoryl group in the transition state for yeast OMP decarboxylase. *Bioorg. Chem.* **2005**, *33*, 45−52.
(30) Warshel, A.; Sharma, P. K.; Kato, M.; Parson, W. W. Modeling electrostatic effects in proteins. *Biochim. Biophys. Acta, Proteins Proteomics* **2006**, *1764*, 1647−1676.
(31) Warshel, A. Electrostatic Origin of the Catalytic Power of Enzymes and the Role of Preorganized Active Sites. *J. Biol. Chem.* **1998**, *273*, 27035−27038.
(32) Stanton, C. L.; Kuo, I. F.; Mundy, C. J.; Laino, T.; Houk, K. N. QM/MM metadynamics study of the direct decarboxylation mechanism for orotidine-5′-monophosphate decarboxylase using two different QM regions: acceleration too small to explain rate of enzyme catalysis. *J. Phys. Chem. B* **2007**, *111*, 12573−12581.

DOI: 10.1021/acs.accounts.8b00059
Acc. Chem. Res. 2018, 51, 960−969

(33) Begley, T. P.; Ealick, S. E. Enzymatic reactions involving novel mechanisms of carbanion stabilization. *Curr. Opin. Chem. Biol.* **2004**, *8*, 508−515.
(34) Smiley, J. A.; DelFraino, B. J.; Simpson, B. A. Hydrogen isotope tracing in the reaction of orotidine-5′-monophosphate decarboxylase. *Arch. Biochem. Biophys.* **2003**, *412*, 267−271.
(35) Tsang, W.-Y.; Wood, B. M.; Wong, F. M.; Wu, W.; Gerlt, J. A.; Amyes, T. L.; Richard, J. P. Proton Transfer from C-6 of Uridine 5′-Monophosphate Catalyzed by Orotidine 5′-Monophosphate Decarboxylase: Formation and Stability of a Vinyl Carbanion Intermediate and the Effect of a 5-Fluoro Substituent. *J. Am. Chem. Soc.* **2012**, *134*, 14580−14594.
(36) Amyes, T. L.; Wood, B. M.; Chan, K.; Gerlt, J. A.; Richard, J. P. Formation and Stability of a Vinyl Carbanion at the Active Site of Orotidine 5′-Monophosphate Decarboxylase: pK_a of the C-6 Proton of Enzyme-Bound UMP. *J. Am. Chem. Soc.* **2008**, *130*, 1574−1575.
(37) Goryanova, B.; Goldman, L. M.; Ming, S.; Amyes, T. L.; Gerlt, J. A.; Richard, J. P. Rate and Equilibrium Constants for an Enzyme Conformational Change during Catalysis by Orotidine 5′-Monophosphate Decarboxylase. *Biochemistry* **2015**, *54*, 4555−4564.
(38) Goryanova, B.; Amyes, T. L.; Gerlt, J. A.; Richard, J. P. OMP Decarboxylase: Phosphodianion Binding Energy Is Used To Stabilize a Vinyl Carbanion Intermediate. *J. Am. Chem. Soc.* **2011**, *133*, 6545−6548.
(39) Goryanova, B.; Goldman, L. M.; Amyes, T. L.; Gerlt, J. A.; Richard, J. P. Role of a Guanidinium Cation−Phosphodianion Pair in Stabilizing the Vinyl Carbanion Intermediate of Orotidine 5′-Phosphate Decarboxylase-Catalyzed Reactions. *Biochemistry* **2013**, *52*, 7500−7511.
(40) Amyes, T. L.; Richard, J. P. Primary Deuterium Kinetic Isotope Effects From Product Yields: Rationale, Implementation, and Interpretation. In *Methods in Enzymology*; Michael, E. H., Vernon, E. A., Eds.; Academic Press, 2017; Vol. *596*; pp 163−177.
(41) Toth, K.; Amyes, T. L.; Wood, B. M.; Chan, K.; Gerlt, J. A.; Richard, J. P. Product Deuterium Isotope Effects for Orotidine 5′-Monophosphate Decarboxylase: Effect of Changing Substrate and Enzyme Structure on the Partitioning of the Vinyl Carbanion Reaction Intermediate. *J. Am. Chem. Soc.* **2010**, *132*, 7018−7024.
(42) Toth, K.; Amyes, T. L.; Wood, B. M.; Chan, K.; Gerlt, J. A.; Richard, J. P. Product Deuterium Isotope Effect for Orotidine 5′-Monophosphate Decarboxylase: Evidence for the Existence of a Short-Lived Carbanion Intermediate. *J. Am. Chem. Soc.* **2007**, *129*, 12946−12947.
(43) Richard, J. P.; Tsuji, Y. Dynamics for Reaction of an Ion Pair in Aqueous Solution: The Rate Constant for Ion Pair Reorganization. *J. Am. Chem. Soc.* **2000**, *122*, 3963−3964.
(44) Toth, K.; Amyes, T. L.; Wood, B. M.; Chan, K. K.; Gerlt, J. A.; Richard, J. P. An Examination of the Relationship between Active Site Loop Size and Thermodynamic Activation Parameters for Orotidine 5′-Monophosphate Decarboxylase from Mesophilic and Thermophilic Organisms. *Biochemistry* **2009**, *48*, 8006−8013.
(45) Harris, P.; Navarro Poulsen, J.-C.; Jensen, K. F.; Larsen, S. Structural basis for the catalytic mechanism of a proficient enzyme: Orotidine 5′-monophosphate decarboxylase. *Biochemistry* **2000**, *39*, 4217−4224.
(46) Harris, P.; Poulsen, J. C.; Jensen, K. F.; Larsen, S. Substrate binding induces domain movements in orotidine 5′-monophosphate decarboxylase. *J. Mol. Biol.* **2002**, *318*, 1019−1029.
(47) Wu, N.; Mo, Y.; Gao, J.; Pai, E. F. Electrostatic stress in catalysis: structure and mechanism of the enzyme orotidine monophosphate decarboxylase. *Proc. Natl. Acad. Sci. U. S. A.* **2000**, *97*, 2017−2022.
(48) Fujihashi, M.; Ishida, T.; Kuroda, S.; Kotra, L. P.; Pai, E. F.; Miki, K. Substrate distortion contributes to the catalysis of orotidine 5′-monophosphate decarboxylase. *J. Am. Chem. Soc.* **2013**, *135*, 17432−17443.
(49) Lewis, C. A.; Wolfenden, R. Orotic Acid Decarboxylation in Water and Nonpolar Solvents: A Potential Role for Desolvation in the Action of OMP Decarboxylase. *Biochemistry* **2009**, *48*, 8738−8745.
(50) Porter, D. J. T.; Short, S. A. Yeast Orotidine-5′-Phosphate Decarboxylase: Steady-State and Pre-Steady-State Analysis of the Kinetic Mechanism of Substrate Decarboxylation. *Biochemistry* **2000**, *39*, 11788−11800.
(51) Vardi-Kilshtain, A.; Doron, D.; Major, D. T. Quantum and Classical Simulations of Orotidine Monophosphate Decarboxylase: Support for a Direct Decarboxylation Mechanism. *Biochemistry* **2013**, *52*, 4382−4390.
(52) Warshel, A.; Strajbl, M.; Villa, J.; Florian, J. Remarkable Rate Enhancement of Orotidine 5′-Monophosphate Decarboxylase Is Due to Transition-State Stabilization Rather Than to Ground-State Destabilization. *Biochemistry* **2000**, *39*, 14728−14738.

DOI: 10.1021/acs.accounts.8b00059
Acc. Chem. Res. 2018, 51, 960−969